NATIONAL AERONAUTICS AND SPACE ADMINISTRATION

Technical Report 32-1261

Theory of Laminar Flames in Stagnation Flows

Raymond Kushida

JET PROPULSION LABORATORY

CALIFORNIA INSTITUTE OF TECHNOLOGY

PASADENA, CALIFORNIA

July 15, 1968

NATIONAL AERONAUTICS AND SPACE ADMINISTRATION

Technical Report 32-1261

Theory of Laminar Flames in Stagnation Flows

Raymond Kushida

Approved by:

D. F. Dipprey, *Manager*
Liquid Propulsion Section

JET PROPULSION LABORATORY
CALIFORNIA INSTITUTE OF TECHNOLOGY
PASADENA, CALIFORNIA

July 15, 1968

TECHNICAL REPORT 32-1261

Prepared Under Contract No. NAS 7-100
National Aeronautics & Space Administration

Contents

Figures

Abstract

The theory of laminar flames sustained in a burner where combustibles are injected through two parallel, opposed porous walls is considered. For steady flow at low Mach numbers, similar solutions of the type found applicable to stagnation flow permit the reduction of the general equations of change to a set of one-dimensional equations. The classic one-dimensional flame equations of Hirschfelder are obtained in a limiting case where the rate of injection from one surface is just equal to the rate of suction at the other surface.

Several examples of combustion experiments done in an apparatus which seems to approximate the ideal configuration have been previously reported. The flat flame diffusion burner of Pandya and Weinberg was the prototype burner on which the analysis was based. However, several other burners not previously recognized to exhibit similar solutions are pointed out. One example is the premixed flat flame burner in which there is flow divergence because of a screen or flat plate placed in the burnt gas flow. The experiments of Schultz where solid pellets are vaporized by pressing against a hot plate can be analyzed by this technique.

Theory of Laminar Flames in Stagnation Flows

I. Introduction

The steady laminar one-dimensional flame has a special importance in basic combustion research because of the relative ease with which rigorous investigations, both theoretical and experimental, can be carried out (see, for example, Ref. 1). The usual configuration of the ideal one-dimensional burner, whose experimental prototypes were developed by Powling (Ref. 2) and by Botha and Spalding (Ref. 3), has the velocity vector always parallel to one of the spatial axes, and properties are uniform in the planes normal to that axis. This classic configuration is limited in utility in that only slow burning or highly cooled flames of premixed combustible gases can be stabilized, and also because the most significant combustion parameter measurable with it is the flame speed. In view of these limitations, it seems worthwhile to explore the possibilities of another class of burner configuration which retains the advantage of a rigorous theory in one dimension, includes diffusion flames as well as premixed flames, and can be reasonably well approximated in laboratory apparatus.

The configuration which has these properties is the parallel porous wall burner. The experimental prototype on which the present theory is based is the flat counterflow diffusion flame of Pandya and Weinberg (Ref. 4). The rigorous molecular theory of dilute gases of Hirschfelder (Ref. 5), specialized to the case of steady axisymmetric laminar flow at vanishingly small Mach number, is used as the starting point for the present theory. When the hypothesis of similar solutions of a type familiar in stagnation flow analysis is invoked (Ref. 6), we find the applicable partial differential equations of momentum, mass, energy, and species conservation are reduced to ordinary differential equations.

The partial differential equations applicable to laminar flame propagation are so complex that substantial simplifications are required even for numerical analysis. The reduction of the problem to that of solving a set of ordinary differential equations is almost essential if any realistic set of chemical parameters are to be considered. It is then possible to utilize some powerful modern numerical techniques to obtain solutions.

The introduction of a second surface, parallel to the injecting surface, differentiates this type of stagnation flow from the one familiar to aerodynamicists. The length scale is now fixed by the distance between the surfaces; this, in turn, enables us to define a Reynolds number independent of boundary-layer considerations. As pointed out by Proudman (Ref. 7), the flow configuration is possibly unique in that the position and structure of all viscous layers, internal as well as boundary, can be determined by classic methods of hydrodynamics and boundary-layer theory. This determinacy of both the position and structure of dissipative layers is now extended to laminar flames.

The essential contribution of this investigation is to show the existence of a class of one-dimensional flames which include premixed as well as diffusion flames. The theory is restricted to flows at small Mach numbers, but this is not an important limitation in most laminar flame studies. With this configuration, the interaction of gas-phase combustion reaction with flow can, in principle, be analyzed in an exact manner.

Search of the literature of combustion research reveals several types of experimental apparatus which approximate the theoretical configuration. Experiments at JPL also confirm some of the qualitative conclusions.

II. Burner Description

Two porous disks are situated with the facing surfaces parallel and the centers of the disks on a common axis perpendicular to these surfaces (Fig. 1). The diameter of the disks is taken to be large compared to the gap width. The disks are uniformly permeable so that the mass rate of injection is uniform over each surface. Different reactants can be injected from each surface so that a diffusion flame forms between the disk surfaces. Alternatively, premixed gases can be injected so that laminar flames are established in the gap. The coordinate and velocity conventions are illustrated in Fig. 1. The coordinate parallel to the axis is the z axis with the velocity component w; the radial coordinate is denoted by r, and the velocity component by v.

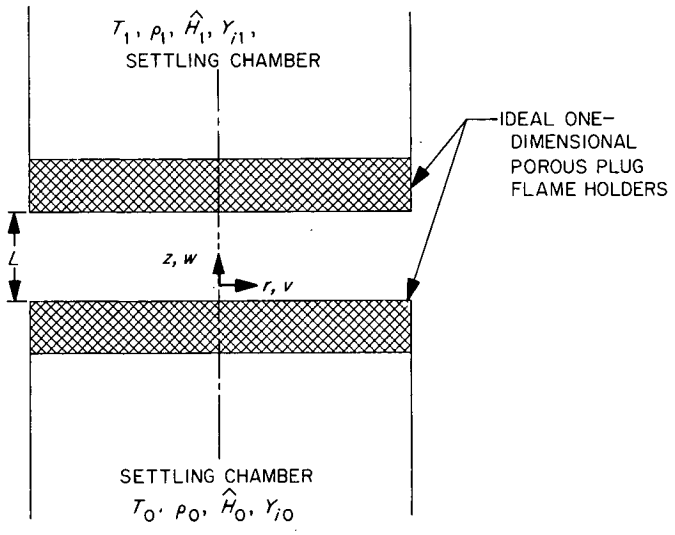

Fig. 1. Schematic diagram of the parallel porous plate burner, illustrating the convention regarding coordinates and velocity components

III. Basic Equations

The partial differential equations for the conservation of mass, momentum, species, and energy are written for steady, laminar, axisymmetric flow. The equations are (Ref. 8):

(1) *For mass*

$$\frac{\partial(\rho v r)}{r\,\partial r} + \frac{\partial(\rho w)}{\partial z} = 0 \tag{1}$$

(2) *For r-wise momentum*

$$\rho v\frac{\partial v}{\partial r} + \rho w\frac{\partial v}{\partial z} + \frac{\partial p}{\partial r} = \frac{\partial \tau_{rr}}{\partial r} + \frac{\partial \tau_{rz}}{\partial z} + \frac{2\mu}{r}\left(\frac{\partial v}{\partial r} - \frac{v}{r}\right) + \rho X_r \tag{2}$$

(3) *For z-wise momentum*

$$\rho v\frac{\partial w}{\partial r} + \rho w\frac{\partial w}{\partial z} + \frac{\partial p}{\partial z} = \frac{\partial \tau_{rz}}{\partial r} + \frac{\partial \tau_{zz}}{\partial z} + \frac{\tau_{rz}}{r} + \rho X_z \tag{3}$$

where we define the viscous stress components as

$$\tau_{rr} = \mu\left[2\frac{\partial v}{\partial r} - \frac{2}{3}(\nabla\cdot\mathbf{v})\right] \tag{4}$$

$$\tau_{rz} = \mu\left[\frac{\partial w}{\partial r} + \frac{\partial v}{\partial z}\right] \tag{5}$$

$$\tau_{zz} = \mu\left[2\frac{\partial w}{\partial z} - \frac{2}{3}(\nabla\cdot\mathbf{v})\right] \tag{6}$$

and the divergence of the velocity vector is

$$\nabla\cdot\mathbf{v} = \frac{\partial v}{\partial r} + \frac{\partial w}{\partial z} + \frac{v}{r} \tag{7}$$

The body forces in the r and z directions are denoted by X_r and X_z, respectively. The equation for the conservation of the ith chemical species is:

$$\frac{\partial[\rho Y_i(v + V_i)r]}{r\,\partial r} + \frac{\partial[\rho Y_i(w + W_i)]}{\partial z} = M_i K_i \tag{8}$$

The diffusion velocities V_i and W_i of the ith chemical species, in the r and z directions, respectively, are defined with respect to the mass average flow velocities. The term Y_i is the mass fraction of the ith species, M_i the

molecular weight, and K_i is the net moles of i created per unit volume per unit time due to chemical reactions.

Lagerstrom (Ref. 6) shows that the kinetic energy and the viscous stress terms can be neglected in gas flows where the Mach number approaches zero. With this restriction the energy conservation equation is

$$\frac{1}{r}\frac{\partial}{\partial r}\left[\rho r\left(v\hat{H}+\sum_{i=1}^{N}V_i\overline{H}_iY_i/M_i\right)-kr\frac{\partial T}{\partial r}+rq_r^{(R)}\right]$$

$$+\frac{\partial}{\partial z}\left[\rho\left(w\hat{H}+\sum_{i=1}^{N}W_i\overline{H}_iY_i/M_i\right)-k\frac{\partial T}{\partial z}+q_z^{(R)}\right]=0 \tag{9}$$

The total enthalpy per unit mass is denoted by $\hat{H}$, $\overline{H}_i$ is the partial molal enthalpy of the ith species, and k is the thermal conductivity. The energy flux due to radiative processes is denoted by $q_z^{(R)}$ and $q_r^{(R)}$. The energy flux due to concentration gradients (Dufour effect) is neglected.

For mixtures of ideal gases, the partial molal enthalpy of the ith species is a function of the temperature alone. The relation for the total enthalpy is then

$$\hat{H}=\sum_{i=1}^{N}\overline{H}_iY_i/M_i \tag{10}$$

where

$$\overline{H}_i=\overline{H}_i^{\circ}(T) \tag{11}$$

The superscript $^{\circ}$ indicates that the partial molal enthalpy is independent of pressure and is a function of temperature alone.

The diffusion velocities are related to the concentration gradients and the binary diffusion coefficients, $\mathcal{D}_{ij}$, by

$$\frac{\partial x_i}{\partial z}=\sum_{j=1}^{N}\frac{x_ix_j}{\mathcal{D}_{ij}}\left[W_j-W_i+\frac{\partial lnT}{\partial z}\left(\frac{D_j^T}{\rho Y_j}-\frac{D_i^T}{\rho Y_i}\right)\right] \tag{12}$$

and

$$\frac{\partial x_i}{\partial r}=\sum_{j=1}^{N}\frac{x_ix_j}{\mathcal{D}_{ij}}\left[V_j-V_i+\frac{\partial lnT}{\partial r}\left(\frac{D_j^T}{\rho Y_j}-\frac{D_i^T}{\rho Y_i}\right)\right] \tag{13}$$

Here the x_i are the mole fractions of the ith species, and D_i^T are the thermal diffusion coefficients. Since there are only $N-1$ independent x_i's, the remaining equations are

$$1=\sum_{i=1}^{N}x_i \tag{14}$$

and

$$0=\sum_{i=1}^{N}Y_iW_i=\sum_{i=1}^{N}Y_iV_i \tag{15}$$

To complete the specification, we state the perfect gas law:

$$p\overline{M}=\rho RT \tag{16}$$

where the mean molecular weight is defined as

$$\overline{M}=\sum_{i=1}^{N}M_ix_i \tag{17}$$

and the relation between mass and mole fractions is

$$Y_i=M_ix_i/\overline{M} \tag{18}$$

At the porous surface, it is assumed that the velocity vector is always normal to the surface. The radial velocity components are therefore zero at the walls. This can be expressed as

$$v(r,0)=v(r,L)=0 \tag{19}$$

where the walls are located on the planes $z=0$ and $z=L$. The mass rates of injection at the walls are given by

$$\rho w(r,0)=\alpha G \tag{20}$$

$$\rho w(r,L)=-(1-\alpha)G \tag{21}$$

Here α is the fraction of the mass flow injected at $z=0$, and G is the net mass flow added per unit area of burner surface per unit time. The negative sign in Eq. (21) is introduced since the velocity $w(r,z)$ is positive when pointed in the positive z direction. We have by addition of Eqs. (20) and (21) the relation

$$\rho w(r,0)-\rho w(r,L)=G \tag{22}$$

which is an expression for the net mass flow G.

In order to simplify the specification of the boundary conditions for species and energy flux, we shall assume that each porous wall is an ideal flameholder of the type considered by Hirschfelder (Ref. 9). This flameholder

prevents the diffusion of active radicals upstream while passing fuel and oxygen freely into the combustion space. It is believed that for any real set of reactions for systems which can be premixed (e.g., H_2–O_2, hydrocarbon–air, etc.), this condition is not required in the present burner system as long as the porous material is not an active catalyst. For a more realistic treatment of the wall boundary condition within the framework of the stagnation flow analysis, it will be necessary only that the boundary conditions be steady in time and be uniform over each surface.

The net mass flux of the ith species at the surfaces is given by the relations

$$[\rho (w + W_i) Y_i] (r, 0) = \alpha G Y_{io} \tag{23}$$

and

$$[\rho (w + W_i) Y_i] (r, L) = -(1 - \alpha) G Y_{iL} \tag{24}$$

where Y_{io} and Y_{iL} are the mass fraction of the ith species in the mixing chambers upstream of the porous surface. For the energy flux, we have correspondingly

$$\left[\rho\left(w\hat{H} + \sum_{i=1}^{N} W_i \overline{H}_i Y_i / M_i\right) - k\frac{\partial T}{\partial z} + q_z^{(R)}\right](r, 0) = \alpha G \hat{H}_o \tag{25}$$

and

$$\left[\rho\left(w\hat{H} + \sum_{i=1}^{N} W_i \overline{H}_i Y_i / M_i\right) - k\frac{\partial T}{\partial z} + q_z^{(R)}\right](r, L) = -(1 - \alpha) G \hat{H}_L \tag{26}$$

where $\hat{H}_o$ and $\hat{H}_L$ are the effective total enthalpy of the gases in the mixing chamber. External heat losses due to conduction can be included as part of the effective total enthalpy. A more complete specification of surface conditions are required to handle radiative energy transfer, but since this is generally only incidental to most combustion problems, we shall leave this open.

The conditions of radial symmetry are used at the axis of the burner. These result in the radial velocity being zero, and all first derivatives of state quantities with respect to r being zero at the position $r = 0$.

It will be convenient in the later analysis to define the stream function $\psi (r, z)$ by the pair of relations

$$\frac{\partial \psi}{\partial z} = \rho v r \tag{27}$$

and

$$\frac{\partial \psi}{\partial r} = -\rho w r \tag{28}$$

The stream functions, as defined by Eqs. (27) and (28), satisfy the mass conservation relation, Eq. (1).

IV. Similarity Transformation

The presence of a stagnation point in the Pandya and Weinberg burner (Ref. 4) suggests that a solution be sought, using the principle of similar solutions (Ref. 10). We pose the following hypotheses:

(1) The stream function, $\psi (r, z)$, is described by a function of the form

$$\psi (r, z) = G r^2 F (z)/2 \tag{29}$$

where G is a constant defined in Eq. (22), and $F (z)$ is a function of z alone.

(2) The static temperature, T, and mass fraction, Y_i, of the ith chemical species are functions of z alone, namely

$$T = T (z) \tag{30}$$

and

$$Y_i = Y_i (z), \qquad i = 1 \cdots N \tag{31}$$

where N is the number of chemical species in the mixture.

We shall test hypotheses (1) and (2) by examining the consequences of adopting them. If the partial differential equations of conservation and the boundary conditions can be satisfied by functions of the form, Eqs. (29), (30), and (31), then obtaining the functions $F (z)$, $T (z)$, and $Y_i (z)$ is tantamount to a full solution. The question as to the uniqueness of the similar solution cannot be answered at this time. We can, however, test the solutions by comparison with experiments.

In the molecular theory of dilute gases, the viscosity, μ, is a function of T and x_i alone; hence, it is a function of z alone. The density is not only a function of T and x_i but also of the static pressure. At the limit of zero Mach number, the variation of pressure must be included in the dynamic terms of Eqs. (1), (2), and (3), but not in the thermal terms of Eq. (16), (Ref. 6). Hence we shall impose the condition that the Mach numbers in the flow field be small compared to unity, which allows us to assume that the density, ρ, is a function of T and x_i, alone.

Body forces can be included if the force vector is parallel to the z axis. In the following analysis, we shall consider only gravity as a body force.

Radiative energy transport is included in the formulation. The radiative properties can be considered a function only of the identity of the molecular species, the temperature, concentration, and static pressure. Again, to the approximation that pressure gradients are insignificant in thermodynamic quantities, we can use a mean pressure to specify the effect of pressure on emissivity. From these considerations, the radiative transfer can be reduced to a problem with a plane-parallel geometry.

From the equations defining the stream functions, Eqs. (27) and (28), and from the formulation of hypotheses (1), we get the relations for the velocity components v and w as

$$v = \frac{Gr}{2\rho}\frac{dF}{dz} \tag{32}$$

and

$$w = -GF/\rho \tag{33}$$

Using these expressions in Eqs. (2) to (7), the momentum equations can be brought into the form

$$\frac{\partial p}{\partial r} = \frac{Gr}{2}\left\{\frac{d}{dz}\left[\mu\frac{d}{dz}\left(\frac{1}{\rho}\frac{dF}{dz}\right)\right] + GF\frac{d}{dz}\left(\frac{1}{\rho}\frac{dF}{dz}\right) - \frac{G}{2\rho}\left(\frac{dF}{dz}\right)^2\right\} \tag{34}$$

and

$$\frac{\partial p}{\partial z} = \frac{G}{\rho}\left[\frac{2}{3}\mu\frac{d^2F}{dz^2} - GF\frac{dF}{dz} + \left(GF^2 - \frac{2}{3}\mu\frac{dF}{dz}\right)\frac{1}{\rho}\frac{d\rho}{dz} - \frac{1}{3}\frac{dF}{dz}\frac{d\mu}{dz}\right] + \rho g \tag{35}$$

where g is the acceleration due to gravity. Noting that G, ρ, μ, F, and g are either constant or at most a function of z alone, the partial differentiation of Eq. (35), with respect to the independent variable r, leads to the result

$$\frac{\partial^2 p}{\partial r \partial z} = 0 \tag{36}$$

Since the static pressure, p, is a state property, it must be expressible as a function $p = p(r, z)$. It follows that the mixed second partial derivative of p must be identical irrespective of the order of differentiation. The partial differentiation of Eq. (34) with respect to z must be identically equal to zero (Eq. 36), but this implies the condition that the term within the braces of Eq. (34) must be a constant. We have, therefore,

$$\frac{\partial p}{\partial r} = \text{constant} \times \left(\frac{Gr}{2}\right) \tag{37}$$

and

$$\frac{d}{dz}\left[\mu\frac{d}{dz}\left(\frac{1}{\rho}\frac{dF}{dz}\right)\right] + GF\frac{d}{dz}\left(\frac{1}{\rho}\frac{dF}{dz}\right) - \frac{G}{2\rho}\left(\frac{dF}{dz}\right)^2 = \text{constant} \tag{38}$$

where the constants in the last two equations are the same. This last equation defines the function for $F(z)$.

The boundary conditions, Eqs. (19), (20), and (21), are transformed by Eqs. (32) and (33) into the corresponding conditions

$$F(0) = -\alpha \tag{39}$$

$$F(L) = 1 - \alpha \tag{40}$$

$$\frac{dF}{dz}(0) = 0 \tag{41}$$

$$\frac{dF}{dz}(L) = 0 \tag{42}$$

If μ and ρ are known as functions of z, then the third-order ordinary differential Eq. (38) can be solved, including the evaluation of the unknown constant, by using conditions, Eqs. (39) to (42). A general analytic solution is not possible, but certain limiting solutions will be discussed later.

We now proceed to treat the species and energy conservation relations using hypothesis (1) and (2). From

hypothesis (2), we find that gradients of temperature and composition in the radial direction vanish, hence the diffusion velocity in the radial direction, V_i, must be identically zero. We need not consider Eq. (13) further.

It will be convenient to define a symbol for the mass flux of the ith species in the z direction as

$$n_i = \rho Y_i (w + W_i) \tag{43}$$

From consideration of hypothesis (2), Eqs. (13), and (33), it is evident that n_i is a function of z alone. Using Eqs. (1), (33), and (43), Eq. (8) can be written as

$$\frac{dn_i}{dz} = M_i K_i - G Y_i \frac{dF}{dz} \tag{44}$$

where the term for the rate of creation of species i, K_i, is a function of ρ, T, and x_i alone. Equation (12) becomes

$$\frac{dx_i}{dz} = \sum_{j=1}^{N} \frac{x_i x_j}{\rho \mathcal{D}_{ij}} \left(\frac{n_j}{Y_j} - \frac{n_i}{Y_i} \right) + k_i^T \frac{d \log T}{dz} \tag{45}$$

where we have defined the thermal diffusivity ratio k_i^T, as

$$k_i^T = \sum_{j=1}^{N} \frac{x_i x_j}{\rho \mathcal{D}_{ij}} \left(\frac{D_j^T}{Y_j} - \frac{D_i^T}{Y_i} \right) \tag{46}$$

This factor is generally important only where temperature gradients are large and the molecular weight of the ith species is greatly different from the average molecular weight of the mixture.

In an analogous way, using Eqs. (1), (33), and (43), the energy Eq. (9) can be brought into the form

$$G \hat{H} \frac{dF}{dz} + \frac{d}{dz} \left(\sum_{i=1}^{N} \frac{n_i \bar{H}_i}{M_i} - k \frac{dT}{dz} + q_z^{(R)} \right) = 0 \tag{47}$$

The boundary conditions at the surface are given by Eqs. (23) to (26) for species and energy flux in the case of the ideal flameholder surface. These are

$$n_i (0) = \alpha G Y_{io} \tag{48}$$

$$n_i (L) = -(1 - \alpha) G Y_{iL} \tag{49}$$

$$\left(\sum_{i=1}^{N} \frac{n_i \bar{H}_i}{M_i} - k \frac{dT}{dz} + q_z^{(R)} \right)_{z=0} = \alpha G H_o \tag{50}$$

$$\left(\sum_{i=1}^{N} \frac{n_i H_i}{M_i} - k \frac{dT}{dz} + q_z^{(R)} \right)_{z=L} = -(1 - \alpha) G \hat{H}_L \tag{51}$$

It will be noted that Eqs. (38), (44), (45), and (47) are a set of ordinary differential equations, which does not contain, explicitly or implicitly, any dependence on the independent variable r. Likewise, the boundary conditions, Eqs. (39) to (42) and Eqs. (48) to (51), are not dependent on r.

The fact that it has been possible to apply hypotheses (1) and (2) in a consistent manner to the original partial differential equations and to the boundary conditions indicates that at least no contradictory situation has arisen. If we can find the functions $F(z)$, $T(z)$, and $x_i(z)$, then these functions will lead to a solution which satisfies all the imposed conditions. We are justified in supposing that the hypothesis of similar solutions will lead to a full solution.

V. Hirschfelder's Flame Equations

The classic equations for one-dimensional laminar flame propagation were described by Hirschfelder (Ref. 9). He considered the velocity vector to be parallel. That case corresponds to the condition that $F(z)$ equals a constant (see Eq. 33). Reference to the boundary conditions, Eqs. (39) and (40), shows this can be obtained only if α, hence $F(z)$, is very much larger than unity. Further, reference to Eq. (33) shows that G must correspondingly be very small, since the velocity, w, must be of the order of the laminar flame speeds. Setting dF/dz equal to zero in Eq. (44) results in the classic species conservation relation. If dF/dz is zero, then the first integral for Eq. (47) is the usual form of the energy-conservation relation. It is evident that the present equations of change for the parallel porous plate burner can be viewed as a more general version of the one-dimensional flame. Unlike the classic one-dimensional case, however, the energy Eq. (47) does not have a simple first integral, so that many of the approximate techniques developed for solving Hirschfelder's equations are not directly applicable.

VI. Stream Function

Comparison of the present formulation of a multidimensional flow in terms of ordinary differential equations with Hirschfelder's problem, outlined in the previous section, shows that the greater generality is gained at the expense of adding a highly nonlinear, essentially fourth-order differential Eq. (38). Since the flow configuration under consideration possesses some unique qualities, we will consider this equation in some detail.

It is convenient to introduce nondimensional parameters. We choose a dimensionless length η defined by

$$d\eta = \rho\, dz/\bar{\rho}L \tag{52}$$

where L is the gap height and $\bar{\rho}$ is a reference density. Choosing $\eta = 0$ at $z = 0$ and $\eta = 1$ at $z = L$, the reference density $\bar{\rho}$ is then defined by

$$\bar{\rho} = \left(\int_0^1 \frac{d\eta}{\rho}\right)^{-1} \tag{53}$$

The viscosity appears as the product, $\rho\mu$. It has been found, for crude analytic treatments, that this product is more nearly a constant than ρ or μ alone. It is convenient to combine this term into a nondimensional group which is defined as

$$C = (\rho\,\mu)/(\bar{\rho}\,\bar{\mu}) \tag{54}$$

and $\bar{\mu}$ is a constant chosen to make C near unity. The Reynolds number N is defined as

$$N = GL/\bar{\mu} \tag{55}$$

Equations (37) and (38) then obtain the form

$$\frac{\partial p}{\partial r} = -\frac{\lambda G^2 r}{4\bar{\rho}L^2} \tag{56}$$

and

$$\frac{1}{N}\frac{d}{d\eta}\left(C\frac{d^2F}{d\eta^2}\right) + F\frac{d^2F}{d\eta^2} - \frac{1}{2}\left(\frac{dF}{d\eta}\right)^2 + \frac{\lambda}{2}\frac{\bar{\rho}}{\rho} = 0 \tag{57}$$

respectively. Here λ is a constant of integration.

Equation (57) is nearly of the form of the Falkner-Skan equation, obtained in blunt-body stagnation flow and in boundary-layer analysis (Ref. 6). The essential distinction is the presence of the undetermined constant, λ, which is, as seen from Eq. (56), a form of the pressure gradient coefficient. We have four boundary conditions, which are restated as

$$F(0) = -\alpha \tag{58}$$

$$F(1) = 1 - \alpha \tag{59}$$

$$\frac{dF}{d\eta}(0) = 0 \tag{60}$$

$$\frac{dF}{d\eta}(1) = 0 \tag{61}$$

Some insight into the behavior of the dimensionless stream function, $F(\eta)$, can be obtained by examining the case where density and viscosity are constant. We shall consider the analytic solutions for very small Reynolds number and for infinite Reynolds number (i.e., inviscid flow).

At low Reynolds number, the viscous forces dominate over the inertial forces. Equation (57) reduces to

$$\frac{d^3F}{d\eta^3} = -\frac{\lambda N}{2}, \qquad \text{for } N << 1 \tag{62}$$

The solution is

$$F = -2\eta^3 + 3\eta^2 - \alpha \tag{63}$$

and

$$\lambda = 24/N \tag{64}$$

where boundary conditions, Eqs. (58) to (61), are used. If relation Eq. (64) is used in the radial pressure gradient expression, Eq. (56), we see that the pressure gradient is inversely proportional to the Reynolds number. The radial velocity profile is parabolic, showing that the solution corresponds to Pouseille flow.

At very large Reynolds number, Proudman (Ref. 7) has shown that the influence of Reynolds number is restricted to a very small region in the vicinity of the contact plane between the fluids injected from the opposing surfaces. If we go to the limit of infinite Reynolds number, then Eq. (57) becomes

$$2F\frac{d^2F}{d\eta^2} - \left(\frac{dF}{d\eta}\right)^2 + \lambda = 0 \tag{65}$$

This is a second-order equation, but there are four boundary conditions to be satisfied. Since λ is an integration

constant, three constraints are ordinarily all that can be satisfied. Proudman finds that the inviscid solution will exhibit a discontinuity in the second and higher derivations of $F(\eta)$ at the contact surface. Equation (65) is satisfied in each region and the constants evaluated by matching the function, F, and its first derivative, F', at the contact surface. We then get

$$F = \eta^2/\alpha - \alpha, \text{ where } 0 \leqq \eta \leqq \alpha \tag{66}$$

$$F = -(1-\eta)^2/(1-\alpha) + 1 - \alpha, \text{ where } \alpha \leqq \eta \leqq 1 \tag{67}$$

and

$$\lambda = 4 \tag{68}$$

Examination of Eq. (56) shows that in the inviscid case, the radial pressure gradient is independent of Reynolds number as required.

Figures 2 and 3 present plots of F and $dF/d\eta$ for various Reynolds numbers. F is proportional to w and $dF/d\eta$ to v. There are equal injection rates from each wall. It will

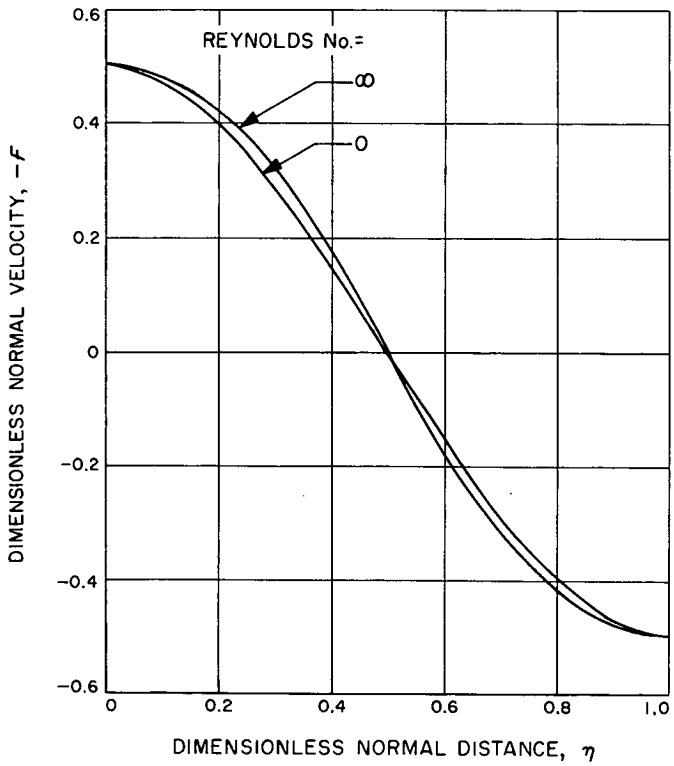

Fig. 2. Velocity normal to plate surfaces; ρ and μ constant; equal blowing rates at each surface

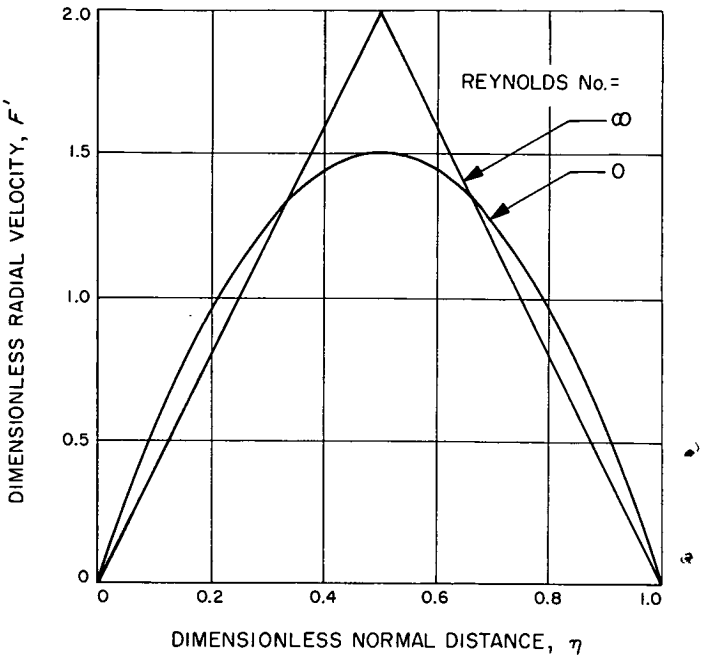

Fig. 3. Radial velocity profile; ρ and μ constant; equal blowing rates at each surface

be noted that the maximum value of $dF/d\eta$ is 1.5 for low Reynolds number and 2.0 for the inviscid case.

In Figs. 4 and 5, F and $dF/d\eta$ are plotted for the case when injection is from one wall (at $\eta = 1.0$) and the other wall is impermeable. At low Reynolds number, the radial velocity profile, as denoted by $dF/d\eta$, is symmetric about the center plane. At higher Reynolds number, the radial velocity profile becomes asymmetric, with the maximum being pushed toward the impermeable wall. The inviscid flow solution is seen to violate the *no-slip* condition at the wall, and the singularity due to the assumption of infinite Reynolds number is evident.

The important aspect of these limiting solutions for the very small and the infinite Reynolds number is that for values of α greater than zero and less 1, the viscous layer is located internal to the flow, away from walls. Proudman states explicitly that while the inviscid solution can possess multiple solutions, the solution with viscosity can possess only one zero in $F(\eta)$, within the range $F(0) = -\alpha$ and $F(1) = 1 - \alpha$. This eliminates the possibility that more than one stagnation point can exist in this flow field. It indicates that Pandya and Weinberg's interpretation of the observation of apparently two stagnation planes in the flow field, when the flame location coincides with the aerodynamic stagnation plane, is in error, as will be discussed later.

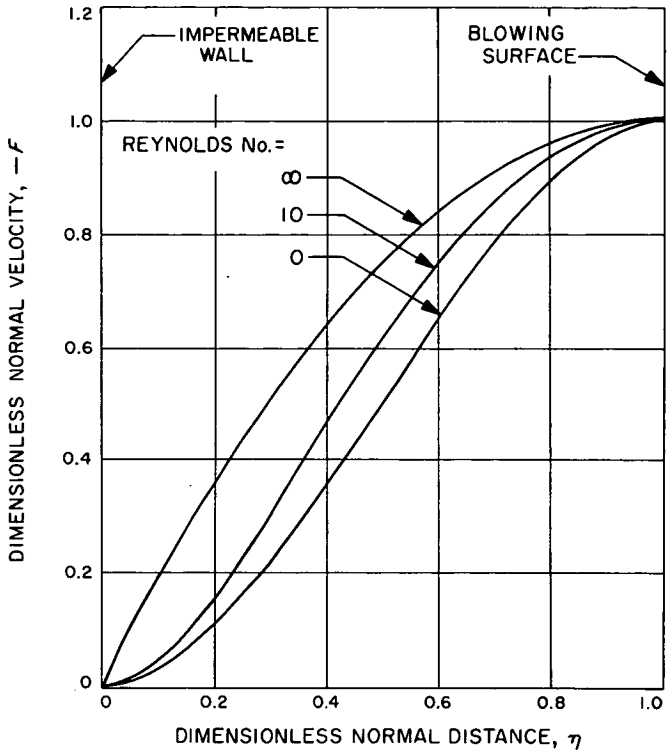

Fig. 4. Velocity normal to plate surfaces; ρ and μ constant; blowing from surface at $\eta = 1$

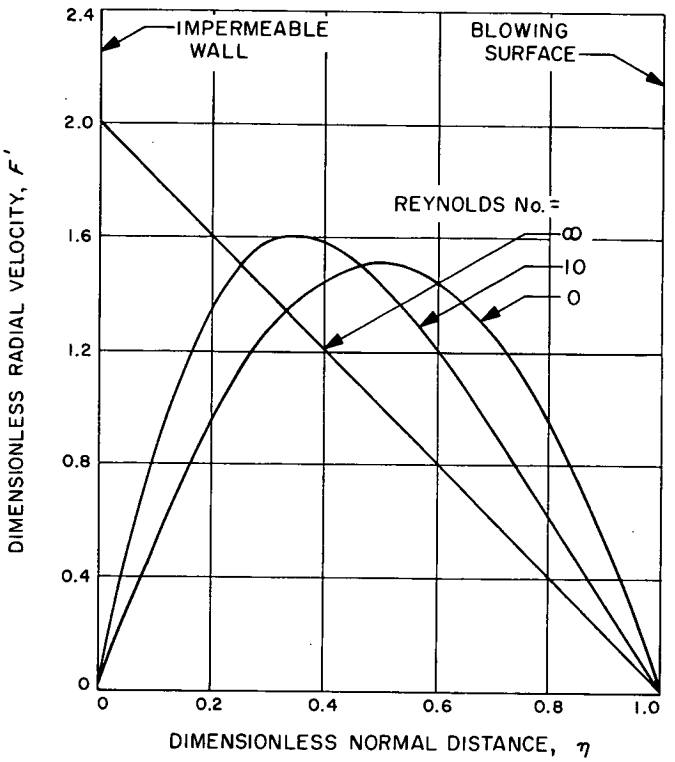

Fig. 5. Radial velocity profile; ρ and μ constant; blowing from surface at $\eta = 1$

VII. Thin Flame

When premixed combustible gases are injected through the porous surfaces, at equal velocities, then two symmetrically placed flat flames will be observed. If the velocity of injection is less than the normal burning velocity, the flame will burn close to the porous surface. Heat loss to the surface allows the actual flame speed to match the injection rate. On the other hand, if the burning velocity is less than the injection velocity at the surface, then the flame will be blown back toward the stagnation point.

To show that the flame will be flat in this latter case, consider the steady laminar flame at the axis, $r = 0$. By symmetry, the flame will be normal to the axis. Since the gas velocity is zero at the stagnation point and higher than the burning velocity at the surface, there will be some intermediate position, say $z = z_u$, where the gas velocity just matches the flame speed. This is the steady state flame position. From relation Eq. (33), the axial component of velocity, w, is a function of z alone and is independent of r. Hence, if the axial velocity, w, is just equal to the burning velocity S_u, at $z = z_u$ and $r = 0$, then $w(r, z_u) = S_u$ at all values of r. From the definition of normal burning velocity, it follows that the flame will be flat and have a definite steady position.

The burning velocity is a meaningful parameter only if the thickness of the flame is small compared to the dimensions of the apparatus. Using an approximate expression (Ref. 11) for the flame thickness, Δ, and normalizing by L the gap height, we have

$$\Delta/L \cong k/C_p\rho_u S_u L = 1/NF_u P_r \qquad (69)$$

where the second equality follows from the definition of Reynolds number, N, and the Prandtl number; we assume Prandtl number to be the order of unity. The symbol F_u denotes the ratio $\rho_u S_u/G$. Thus, the flame will be thin if the F_u ratio is not too small and N is large.

Let us consider a flame of zero thickness. On the unburned side the density is constant at ρ_u and on the burned side the density is ρ_b. Consistent with the thin-flame requirement where N is large, we shall use the inviscid approximation to the flow field.

In Fig. 6 we show the dimensionless axial velocity, F, and radial velocity, $dF/d\eta$, as functions of z/L. The F_u

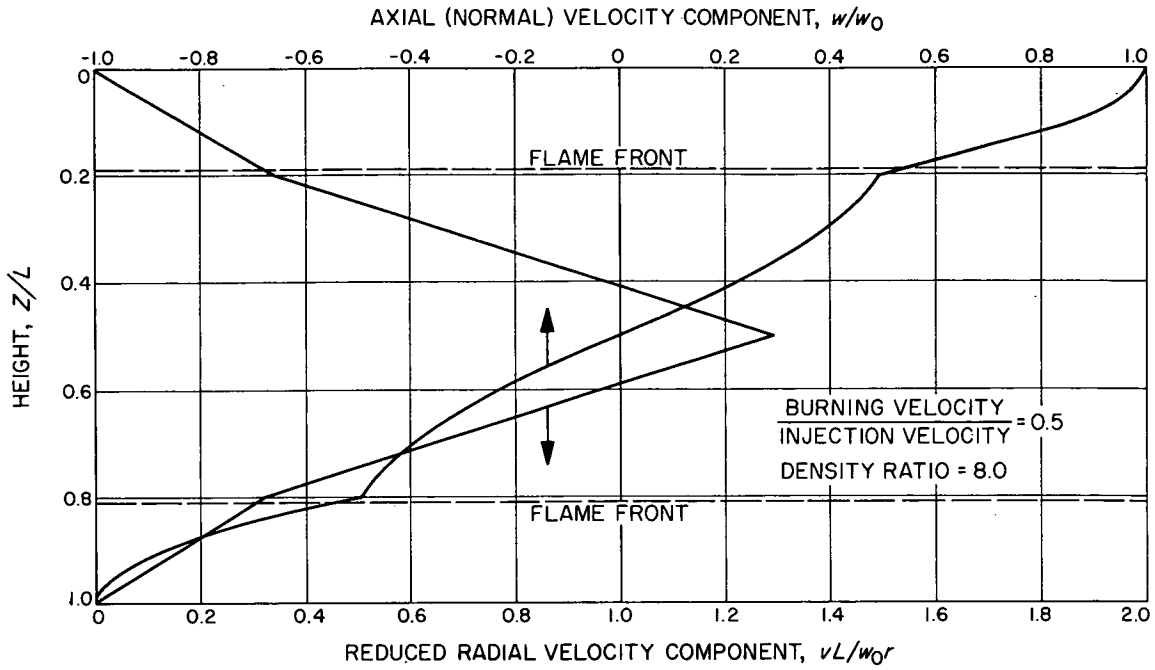

Fig. 6. Radial and axial velocity profiles

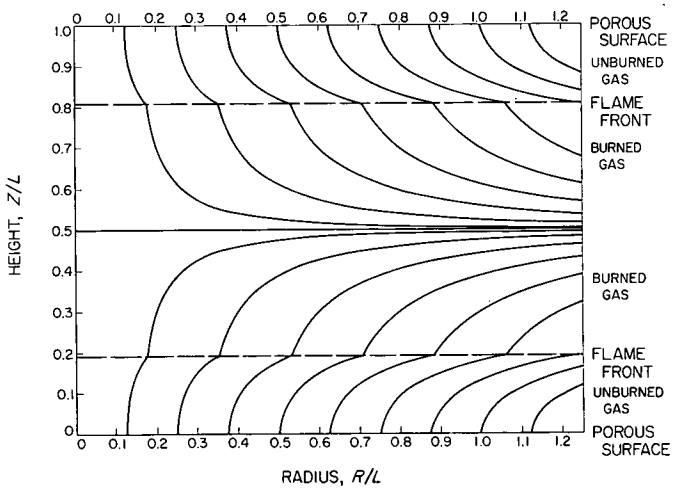

Fig. 7. Streamlines in the opposed flow burner; burning velocity/injection velocity = 0.5; density ratio = 8.0

is taken to be 0.5 and the density ratio, ρ_u/ρ_b, is 8. Note that the coordinate is the dimensionless distance in the physical plane. In Fig. 7, the streamlines are depicted in the r–z plane.

VIII. Experimental Comparison

The analysis for a thin flame in the parallel porous plate burner shows two flat flame fronts located parallel to the surfaces. In Fig. 8, a photograph of a premixed ethylene–oxygen flame in an experimental burner is shown. The

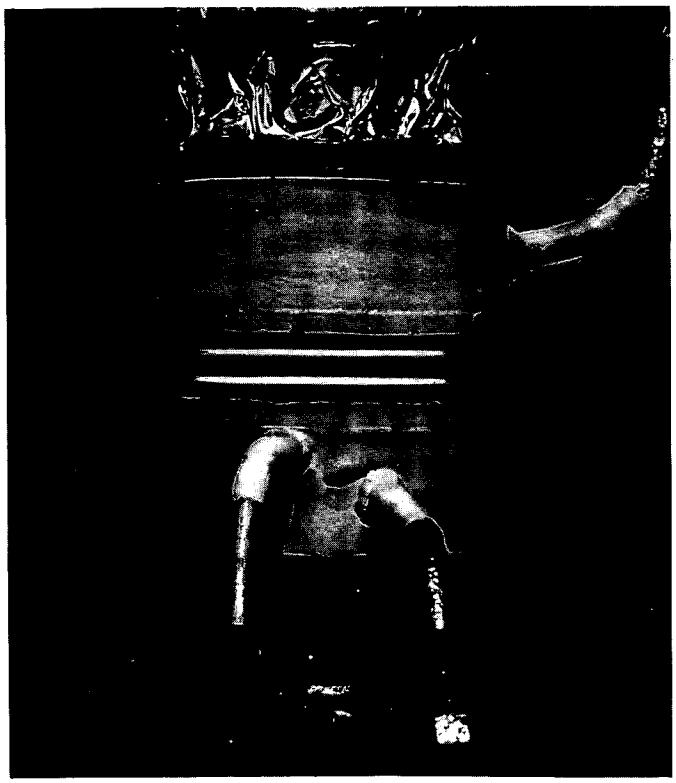

Fig. 8. Premixed ethylene-oxygen-nitrogen flame in a parallel porous plate burner; porous plate diameter: 2 in.; total volumetric flow rate: 70 cm³/s; composition: $C_2H_4/3O_2/6N_2$; chamber pressure: 100 torr

flame is very steady, except for flickering very near the blowout limit.

Pandya and Weinberg (Ref. 4) have made a detailed study of the velocity and temperature field for an ethylene–air diffusion flame in their counter-flow burner. A detailed comparison of their data with the present theory will be published later. The results are in qualitative agreement since the radial velocity component increases linearly with radius and its profile is similar. An anomalous observation on their flame is that when the flame front is made to coincide in location with the aerodynamic stagnation plane, particles do not penetrate into the flame. They discuss this result in terms of two stagnation points separated by a zone with a weak gas source; this interpretation violates the principle of mass conservation. The possibility of multiple zeros in the $F(z)$ function has been discussed by Proudman (Ref. 7). He proves that, in the case of constant density flow, $F(z)$ can have at most one zero. The introduction of density and viscosity variation in Eq. (38) will not alter this conclusion. The explanation for the particle track observations will probably be found in thermomechanical effects due to temperature gradients (Ref. 12).

Beidler and Hoelsher (Ref. 13) report an experiment in which a flat flame for premixed propane–air mixture was obtained by placing a large flat plate normal to the flow of the combustion product. The porous surface was a set of screens. This flow is undoubtedly of the stagnation flow type and is an asymmetric version of the flame illustrated in Fig. 8.

Various modifications of the Powling burner (Ref. 2) have been widely used in fundamental combustion research because of its close approximation to the classic, paraxial-flow, laminar flame of theory. In this burner very slow burning mixtures can be made to float stably above a porous surface through which the combustibles flow. However, it is almost always necessary to insert a screen or perforated plate in the burnt gas stream to stabilize its position (Ref. 1). This stability is due to the slight flow divergence caused by the pressure drop of the combustion products flowing through the obstructing screen. Although this type of flow does not have a stagnation point, its solution, nevertheless, is contained in the family of flows discussed in this paper. In this case, one surface injects gas while the other surface sucks gas. Comparison of Eqs. (20), (21), and (22) make it clear that this condition corresponds to the parameter α being larger than unity (where injection occurs at $z = 0$). The degree of flow divergence decreases as α becomes larger. As shown previously in the limit where α approaches infinity, Hirschfelder's equations were obtained. However, in this limit, the position of the flame is no longer determinate. Experimentally, this fact seems to manifest itself by the inability to obtain a truly flat flame with paraxial flow except by partial quenching (this latter type of flat flame has been used first by Botha and Spalding, Ref. 3).

An experimental study of interest to combustion research, even though combustion reactions are not involved, is that of Schultz (Ref. 14). He measured the surface regression velocity for the vaporization of ammonium salts by pressing pellets against a hot plate with a known force and known plate-surface temperature. Nachbar and Williams (Ref. 15) have presented a theoretical analysis for the gas film formed by the subliming solid, which acts as a thermal resistance to the transfer of heat from plate to solid. However, they were forced to leave undetermined the question of the thickness of the gas film. With the aid of the theory of stagnation flows, the effect of the applied force, pellet diameter, and gas properties can be used to predict the gas film thickness. It will not be necessary to perform modified experiments of the type suggested by Nachbar and Williams since Schultz's experimental configuration is already very nearly ideally suited to analysis. Chaiken et al. (Ref. 16) and Cantrell (Ref. 17) have given simplified treatments of the gas film flow, in which some of the essential features of the present analysis are utilized.

IX. Application to Combustion Research

The development of a rigorous one-dimensional theory for the parallel porous plate configuration leads to the possibility of many new types of theoretical and experimental investigation of combustion phenomena. The inherent advantage of the configuration is due to the introduction of a second porous surface, parallel to the first. The second surface can be used in suction or in injection, as a blank wall or as a plane of symmetry. Both diffusion flames and premixed flames, and surface interactions of flames can be treated within the framework of the theory.

It is believed that the boundary conditions are sufficiently unrestrictive so that a number of phenomena which have been rather difficult to treat analytically now become mathematically somewhat more tractable, especially in view of the capabilities of modern computers. These phenomena can include surface catalysis, surface vaporization, and heat loss due to conduction and due to radiation. It is felt that with the well-posed boundary

conditions inherent in this configuration, new insight into problems of flammability limits can be obtained.

It is well known that flame propagation limits are reached at finite burning velocities because of heat losses. In our preliminary experiments with the porous plate burner, this phenomena is very evident since the two symmetrically placed flame fronts (see Fig. 8) approach each other but do not quite merge as the flammability limit is approached. The comparison of a theoretical analysis of the extinction limit and experiment would be of interest in combustion research.

An exact one-dimensional configuration for diffusion flames with convection is important since many systems of practical interest cannot be premixed with safety. It is expected the blowout, quenching, and ignition can be observed in this configuration. A new experimental study of hydrazine–nitrogen tetroxide ignition with an apparatus designed along these principles is being initiated. It is expected that quantitative evaluation of the thermal reactions leading to ignition will be obtained.

Substantial contributions from combustion researchers to the general fund of knowledge concerning high temperature chemical reactions were rare until Powling or the Botha and Spalding burner became widely used. It is hoped that with this new type of laminar flame burner, research into combustion reactions can be extended into new areas.

Nomenclature

C	$\rho\mu/\bar{\rho}\bar{\mu}$, dimensionless
C_p	mean specific-heat capacity at constant pressure, joules/g/°K
D_i^t	thermal diffusion coefficient, g/cm/s
$\mathcal{D}_{ij}$	binary diffusion coefficient, cm²/s
F	dimensionless stream function
G	net injected mass flux, g/cm²/s
H	total enthalpy, joules/g
$\overline{H}_i$	partial molal enthalpy, joule/g-mol
K_i	rate of reaction, g-mol/cm³/s
k	thermal conductivity, joule/cm/°K/s
k_{ti}^t	thermal diffusion ratio, dimensionless
L	gap height, cm
M_i	molecular weight, g/g-mol
$\overline{M}$	mean molecular weight, g/g-mol
N	Reynolds number, dimensionless
N	total number of chemical species, dimensionless
n_i	mass flux of ith species, g/cm²/s
P_r	Prandtl number, dimensionless
p	static pressure, dyn/cm²
$q^{(R)}$	energy flux due to radiation, joule/cm²/s
R	gas constant, joule/g-mol/°K
r	radial coordinate, cm
S_u	normal burning velocity, cm/s
T	temperature, °K
V_i	r component of diffusion velocity relative to mass average velocity, cm/s
v	r component of mass average velocity, cm/s
W_i	z component of diffusion velocity relative to mass average velocity, cm/s
w	z component of mass average velocity, cm/s
X	body force, cm/s²
X_i	mole fraction
Y_i	mass fraction
z	length coordinates
α	fraction of mass flow injected
η	dimensionless coordinate in the z-wise direction
λ	dimensionless constant
μ	viscosity, g/cm/s
ρ	density, g/cm³
τ_{ij}	stress tensor component, dyn/cm²
ψ	stream function

References

1. Fristrom, R. M., and Westenberg, A. A., *Flame Structure*, McGraw-Hill Book Company, New York, 1965.
2. Powling, J., *Fuel*, *28*, 25–28, 1949.
3. Botha, J. P., and Spalding, D. B., *Proc. Roy. Soc.* (London), *A 225*, 71, 1954.
4. Pandya, T. P., and Weinberg, F. J., *Proc. Roy. Soc.* (London), *A 279*, 544–561, 1964.
5. Hirschfelder, J. O., Curtiss, C. F., Bird, R. B., *Molecular Theory of Gases and Liquids*, J. Wiley and Sons, N. Y., 1954.
6. Lagerstrom, P., "Section B—Laminar Flow Theory," pp. 20–285, *Theory of Laminar Flows*, ed. F. K. Moore, Princeton University Press, Princeton, New Jersey, 1964.
7. Proudman, I., *J. Fluid Mechanics*, *9*, 593, 1960.
8. Bird, R. B., Steward, W. E., Lightfoot, E. N., *Transport Phenomena*, J. Wiley and Sons, N. Y., 1960.
9. Hirschfelder, J. O., and Curtiss, C. F., *Third Symposium on Combustion and Flame and Explosion Phenomena*, pp. 121–127, Williams and Wilkins Company, Baltimore, Maryland, 1949.
10. Ames, W. F., *Nonlinear Partial Differential Equations in Engineering*, Academic Press, N. Y., 1965.
11. Williams, F. A., *Combustion Theory*, Addison–Wesley Publishing Company, Reading, Massachusetts, 1965.
12. Mason, E. A., and Monchick, L., *Ninth Symposium (International) on Combustion*, pp. 713–724, Academic Press, N. Y., 1963.
13. Beidler, W. T., III, and Hoelscher, H. E., *Jet Propulsion*, *27*, 1257–1260, 1957.
14. Schultz, R. D., and Dekker, A. O., *Fifth Symposium (International) on Combustion*, pp. 260–267, Reinhold, N. Y., 1955.
15. Nachbar, W., and Williams, F. A., *Ninth Symposium (International) on Combustion*, pp. 345–357, Academic Press, N. Y., 1963.
16. Chaiken, R. F., Sibbett, D. H., Sutherland, J. E., Van der Mark, D. K., and Wheeler, A., *J. Chem. Phys.*, *37*, 2311–2318, 1962.
17. Cantrell, R. H., *AIAA Journal*, *1*, 1544–1550, 1963.